Electronic Supplementary Material (ESI) for RSC Advances.

## Supplementary Information

# Stabilization and Transformation of Pt Nanocrystals Supported on $ZnAl_2O_4$ Spinel

Wei-Zhen Li,[†,#] Libor Kovarik,[†] Yingwen Cheng,[†] Lei Nie,[†] Mark Bowden,[†] Jun Liu,[†,*] Yong Wang[†,‡,*]

[†] Institute for Integrated Catalysis, Pacific Northwest National Laboratory, P.O. Box 999, Richland, WA 99352, USA.

[‡] The Gene & Linda Voiland School of Chemical Engineering and Bioengineering, Washington State University, Pullman, WA 99164, USA.

E-mail: yong.wang@pnnl.gov; jun.liu@pnnl.gov

# Present Addresses: State Key Laboratory of Catalysis, Dalian Institute of Chemical Physics, Chinese Academy of Sciences, Dalian, 116023, China. E-mail: weizhenli@dicp.ac.cn

## Experimental details:

**Materials synthesis:** Zinc aluminate spinel supports were prepared by hydrolysis of aluminum isopropoxide with zinc nitrate hexahydrate in ethanol (equation 1). Stoichiometric quantities of aluminum isopropoxide (98+%, Alfa Aesar) (0.1 mol) and zinc nitrate hexahydrate (98%, Alfa Aesar) (0.05 mol) were mixed in 300 ml denatured ethanol in a 1000 ml Pyrex bottle. The bottle was sealed and then put on a heating plate with magnetic stirring. After stirring for 1h, the plate was heated to 150 °C and held there for 12 h. Then the ethanol was evaporated and the resultant gel was dried at 90 °C overnight. Finally, the dried powders were calcined in ambient air at 800 °C for 12 h with a heating rate of 5 °C/min, resulting in the formation of $ZnAl_2O_4$ support materials with pure spinel crystal phase. The as-synthesized $ZnAl_2O_4$ powders was also further calcined at 900, 1000, 1050, and 1100 °C for 2 h as have been discussed in the paper, respectively.

$$x\text{Zn(NO}_3)_2\cdot 6\text{H}_2\text{O} + 2x\text{Al(O-}i\text{-Pr)}_3 \rightarrow [\text{Zn-(OH)}_6\text{-Al}_2]_x^{2x+} + 2x\text{NO}_3^- + 6xi\text{-PrOH} \qquad (1)$$

Supported Pt samples were prepared by incipient wetness impregnation of $ZnAl_2O_4$ spinel using aqueous solutions of $PtCl_4$ (99.9%, Alfa Aesar) at room temperature for 20 h. The Pt loading levels were controlled at 1, 3, 5 or 8 wt%. Impregnated samples were dried at 110 °C in ambient air overnight and then treated as follows. They were first calcined at 500 °C for 5 h and then were reduced in 5% $H_2$/He at 800 °C for 2 h. After this high temperature reduction, residual chloride ions in the samples were below the XPS detection limit (0.1% surface atomic ratio). Thus, the influence of $Cl^-$ on reactivity and Pt stability can be neglected. Since severe sintering of Pt usually occurs during long term high temperature treatment in oxidizing atmospheres, the reduced samples were subsequently aged in ambient air at 800 °C for 1 week (168 h, "1W"). The aged samples were also reduced in 5% $H_2$/He at 800 °C for 2 h. We denote the calcining treatment of as "O" and that of $H_2$ reduction as "R". Thus, these samples are designated with a suffix of "-FO" and "-FR", or "-1WO" and "-1WR", respectively.

**Catalyst Characterization:** Surface areas were measured on a QuantaChrome Autosorb-6 using $N_2$ adsorption isotherms and the BET analysis method. All of the samples were degassed under vacuum at 150 °C for 4 h before the adsorption measurements. High-resolution scanning transmission electron microscopy (STEM) imaging was performed with a FEI Titan 80-300 microscope operated at 300 kV. The instrument is equipped with CEOS GmbH double-hexapole aberration corrector for the probe-forming lens, which allows imaging with 0.1 nm resolution. The images were acquired on High Angle Annular Dark Field (HAADF) with inner collection angle of 52 mrad. STEM specimens were prepared by depositing a suspension of the powdered sample on a lacey carbon-coated copper grid. X-ray diffraction (XRD) patterns were measured on a Philips PW3040/00 X'Pert MPD system equipped with a Cu source ($\lambda$ = 1.5406 A). Data analysis was accomplished using JADE$^{®}$ (Materials Data, Inc., Livermore, CA) as well as the Powder Diffraction File database (2003 Release, International Center for Diffraction Data, Newtown Square, PA). Crystallite size and quantitative phase analysis were performed using the Scherrer equation and Rietveld method. Pt dispersions were obtained by hydrogen pulse chemisorption using a thermal conductivity detector (TCD) on a GC-7890A at 50 °C. Before the chemisorption, the sample was heated to 800 °C for 0.5 h under 2% $H_2/N_2$ and switched to $N_2$ and held for 0.5 h, then cooled down to 50 °C in $N_2$.

Table S1. Surface area, Pt dispersion and crystallite size of $ZnAl_2O_4$ and $1Pt/ZnAl_2O_4$ samples.

| Sample | $S_{BET}$ ($m^2/g$) | Average size by XRD (nm) | | | | Fraction (wt%) | | | | Pt dispersion (%) |
|---|---|---|---|---|---|---|---|---|---|---|
| | | Spinel | ZnO | Pt | PtZn | ZnO | Fine Pt | Large Pt | PtZn | |
| $ZnAl_2O_4$ | 110.3 | 12 | | | | | | | | |
| $1Pt/ZnAl_2O_4$-FO | | 18 | 31 | | | 1.3 | | | | |
| $1Pt/ZnAl_2O_4$-FR | 92.4 | 18 | | | | | | | | 40.2 |
| $1Pt/ZnAl_2O_4$-1WO | | 20 | | 97 | | | 0.3 | 0.7 | | |
| $1Pt/ZnAl_2O_4$-1WR | 46.2 | 20 | | | 73 | | 0.3 | | 0.9 | 10.4 |

Table S2. Crystallite sizes and fractions of segregated ZnO of $ZnAl_2O_4$ calcined at different temperatures.

| Sample | Average size by XRD (nm) | | Fractions of ZnO (wt%) |
|---|---|---|---|
| | Spinel | ZnO | |
| $ZnAl_2O_4$-800 | 12 | | |
| $ZnAl_2O_4$-900 | 24 | 32 | 2.6 |
| $ZnAl_2O_4$-1050 | 27 | 30 | 2.4 |
| $ZnAl_2O_4$-1050 | 45 | 42 | 1.9 |
| $ZnAl_2O_4$-1100 | 65 | 45 | 1.0 |
| $ZnAl_2O_4$-1200 | 74 | 54 | 0.3 |

Table S3. Crystallite sizes, ratios of fine and large Pt, fractions of compositions, and lattice constants of segregated γ-$Al_2O_3$ in Pt/$ZnAl_2O_4$ samples. The calculated lattice constants of the "γ-$Al_2O_3$" phase were slightly larger than the standard ones ($c$ = 7.90 Å, PDF#10-0425). Considering there were no detectable Zn containing structures besides the small portions of PtZn that could be counterparts of the segregated "γ-$Al_2O_3$", the "γ-$Al_2O_3$" could be "Zn containing γ-$Al_2O_3$" since similar diffractions can also be displayed if the $Al^{3+}$ in tetrahedral sites were replaced by $Zn^{2+}$. For simplification, we still treat the phase as pure alumina in estimating the fractions since we have no way to know the accurate compositions, leading to less reliable in the absolute value. However, the ratios of fine and large Pt in the samples are reliable.

| Sample | Average size by XRD (nm) | | | Ratio of Pt Fine: Large | Fraction (wt%) | | | $c_{(\gamma\text{-}Al_2O_3)}$ (Å) |
|---|---|---|---|---|---|---|---|---|
| | Spinel | PtZn | γ-$Al_2O_3$ | | Fine Pt | PtZn | γ-$Al_2O_3$ | |
| 5Pt/$ZnAl_2O_4$-FR | 21 | 62 | 11 | 1.04 | 2.5 | 3.2 | 41 | 7.970 |
| 3Pt/$ZnAl_2O_4$-900-FR | 26 | 167 | 11 | 1.63 | 1.1 | 0.9 | 22 | 7.932 |
| 5Pt/$ZnAl_2O_4$-900-FR | 18 | 125 | 14 | 1.15 | 3.2 | 3.7 | 61 | 7.928 |
| 8Pt/$ZnAl_2O_4$-900-FR | 21 | 97 | 13 | 0.98 | 3.9 | 5.3 | 54 | 7.928 |
| 5Pt/$ZnAl_2O_4$-1050-FR | 36 | 137 | 14 | 0.74 | 1.4 | 2.5 | 37 | 7.944 |
| 8Pt/$ZnAl_2O_4$-1050-FR | 22 | 71 | 21 | 1.84 | 3.6 | 2.6 | 63 | 7.924 |

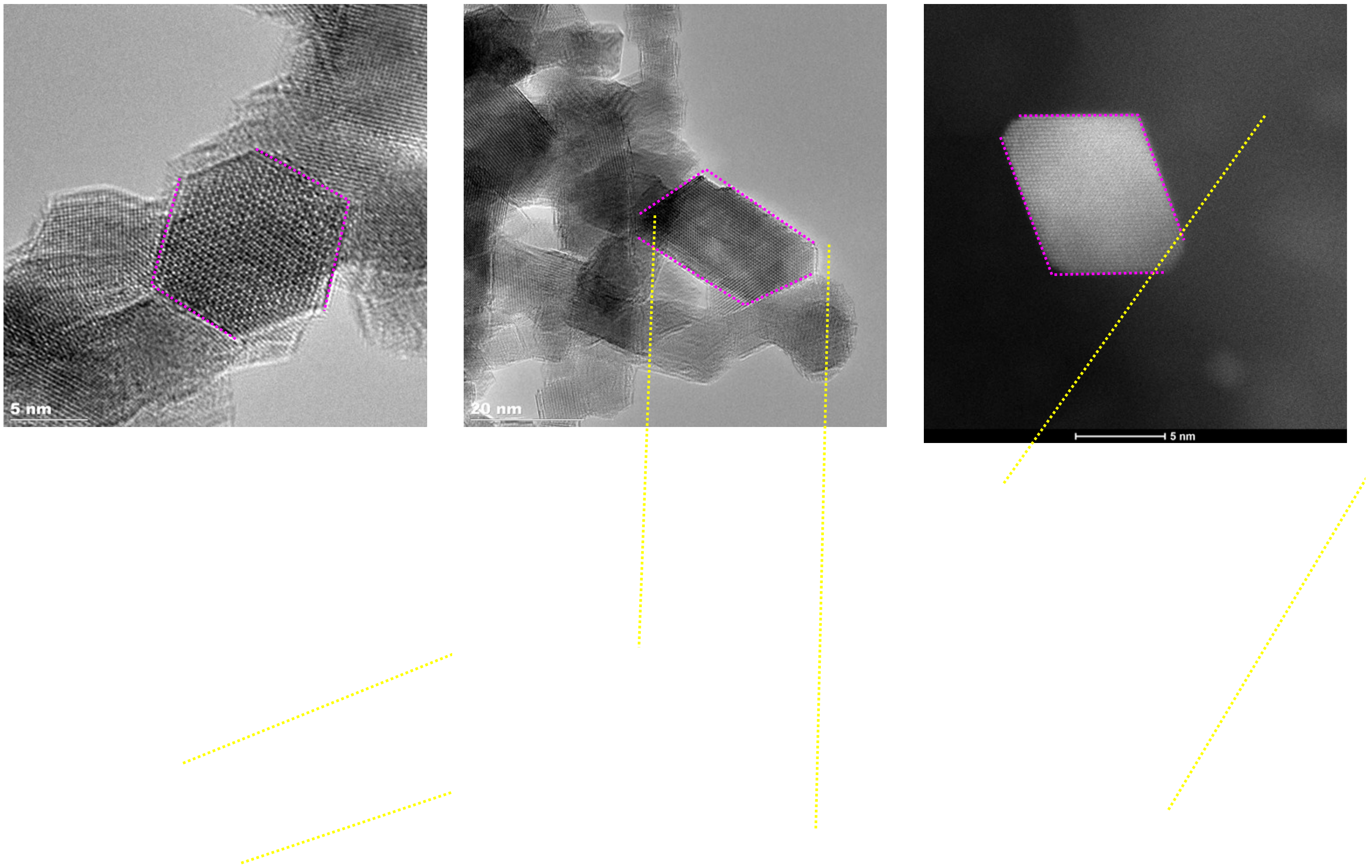

Figure S1. TEM and STEM images for $ZnAl_2O_4$ spinel after calcination at 800 °C. The {111} and {100} facets are marked in magenta and yellow dash lines, respectively. The percentage of {111} in the total surface was estimated to be around 60-90% from the aspect ratios by assuming all the particles are in cuboctahedral shapes with eight {111} and six {100} facets.

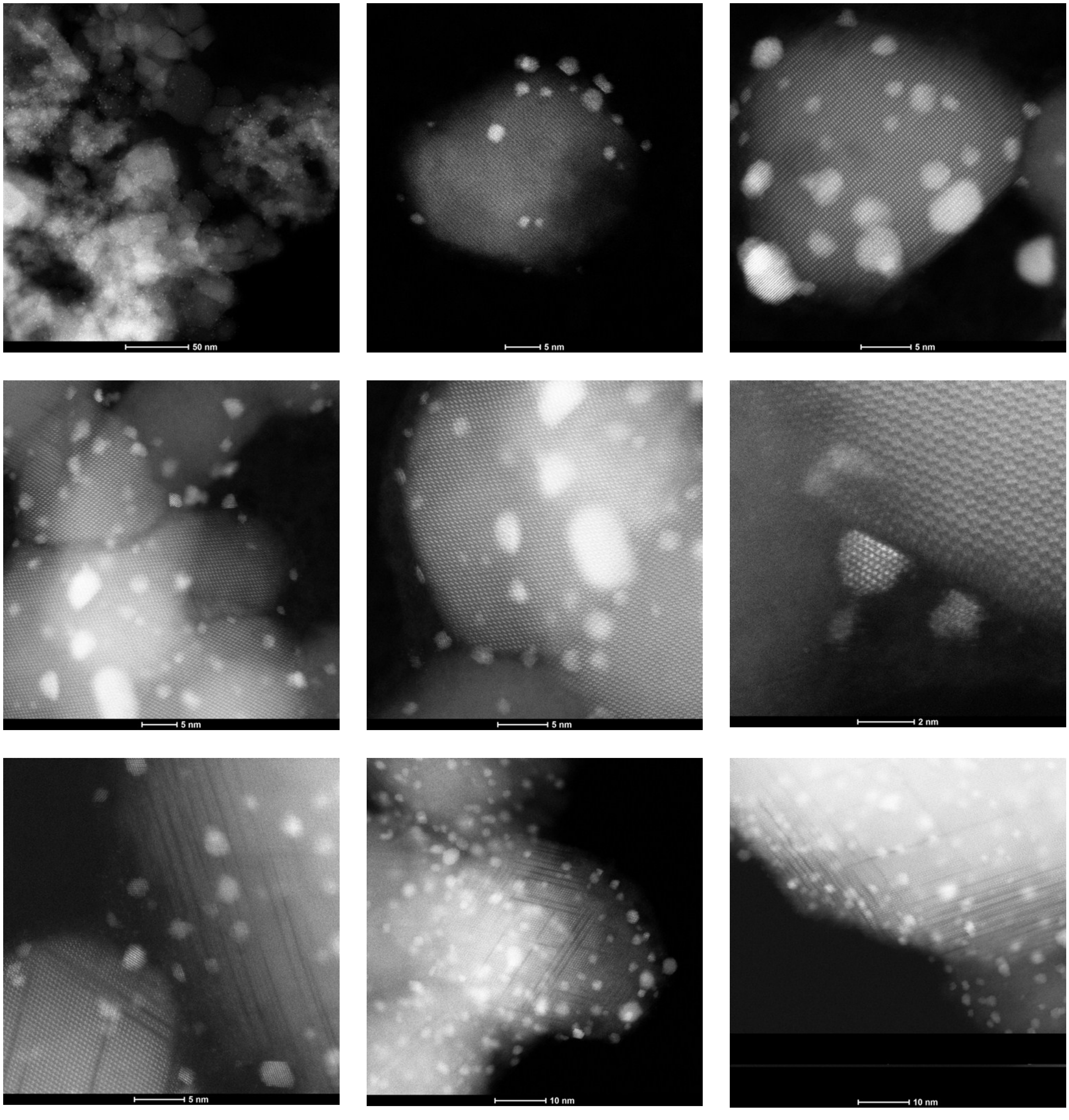

Figure S2. STEM images for 1Pt/$ZnAl_2O_4$-FR which was prepared by calcining impregnated samples at 500 °C for 5 h and then reducing in $H_2$ at 800 °C for 2 h. Small Pt nanoparticles randomly occupy the surfaces of $ZnAl_2O_4$ spinel support. The small particles clearly show characteristics of metallic Pt rather than PtZn alloy. Normal stoichiometric $ZnAl_2O_4$ spinel and non-stoichiometric $ZnAl_2O_4$ spinel nanoparticles with fault (111) planes are both evident.

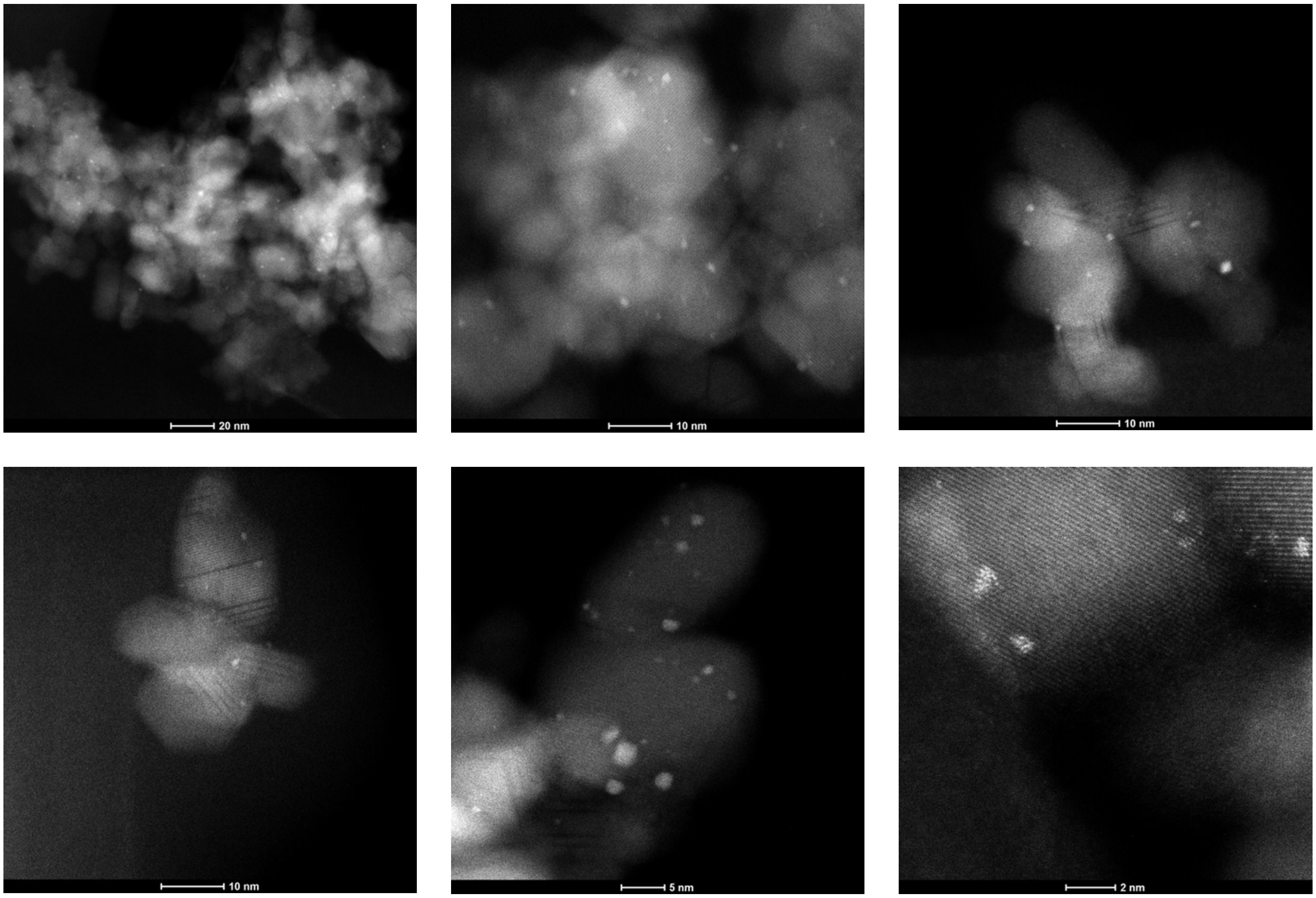

Figure S3. STEM images for 1Pt/$ZnAl_2O_4$-1WR which was aged at 800 °C in air for 7 days and then reduced in $H_2$ at 800 °C for 2 h. Small Pt nanoparticles were evident in most areas of the specimens although the Pt particle density is smaller than that for the 1Pt/$ZnAl_2O_4$-FR sample, illustrating that $ZnAl_2O_4$ spinel has unique surface structure that can stabilize Pt at small sizes during the very severe aging.

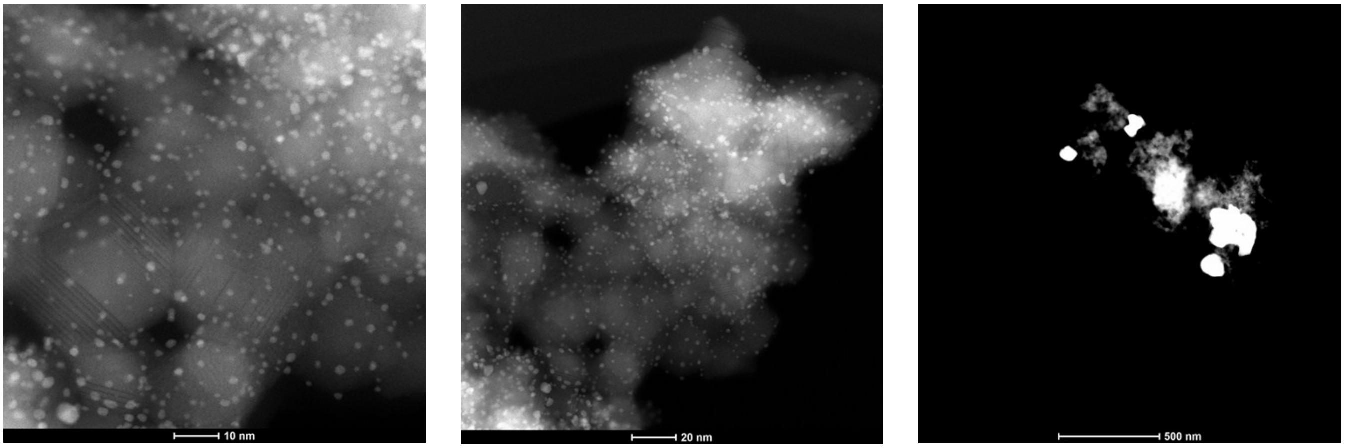

Figure S4. STEM images for 5Pt/$ZnAl_2O_4$-FR which was prepared by calcining impregnated sample at 500 °C for 5 h and then reducing in $H_2$ at 800 °C for 2 h. High Pt loading beyond the dispersion capability leads to formation of large PtZn alloy particles.

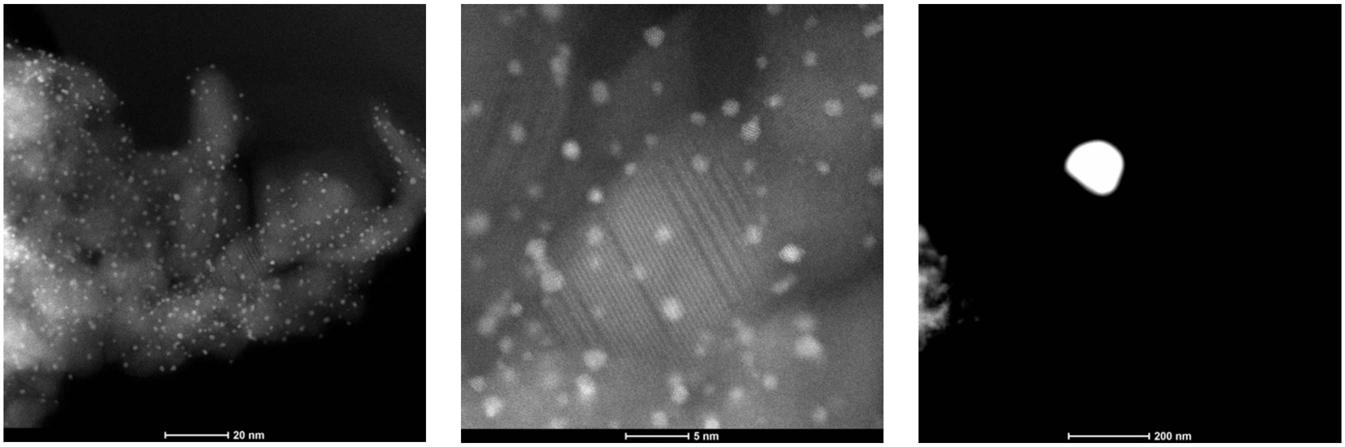

Figure S5. STEM images for 3Pt/$ZnAl_2O_4$-900-FR which was prepared by calcining impregnated sample at 500 °C for 5 h and then reducing in $H_2$ at 800 °C for 2 h.

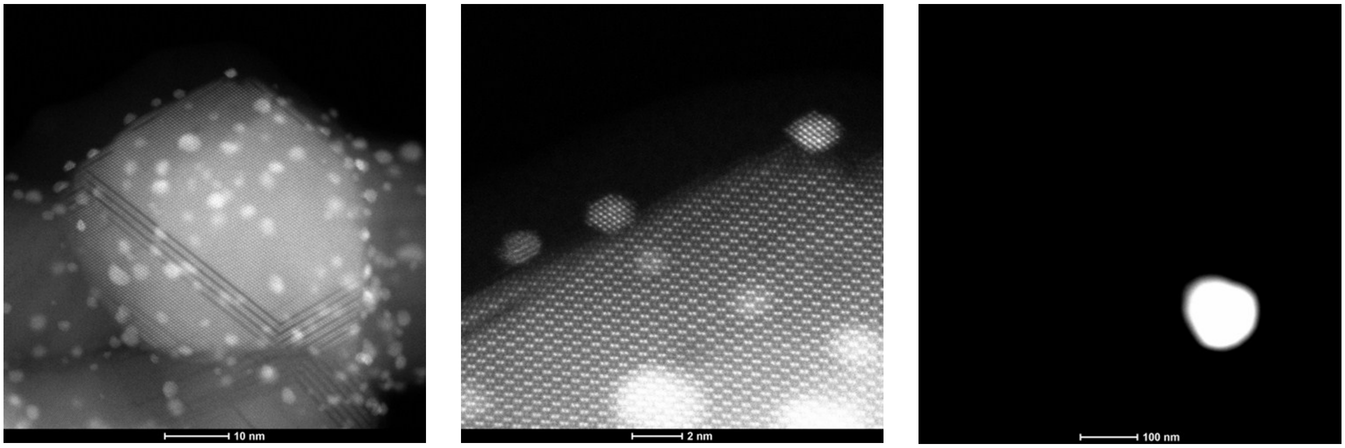

Figure S6. STEM images for 5Pt/$ZnAl_2O_4$-1050-FR which was prepared by calcining impregnated sample at 500 °C for 5 h and then reducing in $H_2$ at 800 °C for 2 h. The small particles clearly show characteristics of metallic Pt rather than PtZn alloy.